COMOTI
ROMANIAN RESEARCH & DEVELOPMENT INSTITUTE FOR GAS TURBINES
220D Iuliu Maniu Ave., 061126 Bucharest 6, ROMANIA PO 76, POB 174
Phone: +4 021/4340198, +4 021/4340240; Fax: +4 021/4340241
E-mail: contact@comoti.ro, www.comoti.ro
Nr. Of. Com. Reg. J40/4880/1997, CIF: RO445238

ESA Contract no. 4000126703/19/NL/BJ/va
- EXECUTIVE SUMMARY REPORT - "Developing metal Additive Manufacturing Expertise to meet the requirements of Space Industry"
Framework: "Assessments to Prepare and De-Risk Technology Developments".
Project Acronym – "SparK"
Period covered: 01.03.2019 – 30.11.2019
Date: 30.11.2019
Edition: 1 | Revision: 0
Prepared by COMOTI

Contents

1. INTRODUCTION

1.1. SCOPE OF THE DOCUMENT

The present document presents the findings within the activity “Developing metal Additive Manufacturing Expertise to meet the requirements of Space Industry”, part of the Framework “Assessments to Prepare and De-Risk Technology Developments”, carried out by the ROMANIAN R&D INSTITUTE FOR GAS TURBINES COMOTI.

1.2. BACKGROUND

Additive Manufacturing technology has evolved rapidly toward developing high finish end, complex shape products, using an environmentally friendly approach. However, the technology presents more challenges compared to the conventional manufacturing technologies, especially regarding the process control and stability. Therefore, it was identified the necessity to establish for each individual machine a process route traceability in order to define the optimum process parameters and to ensure the process repeatability and reliability, combined with the machine capabilities.

Space engineering is a research field where AM technology could be integrated to ensure a reduction of manufacturing costs of the components for space applications the build speed being one of the significant cost drivers for lower production rates. The primary challenge for AM space products is the fulfilment of qualification requirements and the guarantee that all parts lots have the expected mechanical properties and the same high-quality dealing with the effects of thermal induced residual stresses, structural anisotropy and quality, and parts performances.

The present project’s objectives and outcomes are in agreement with ESA’s TRP and GSTP objectives regarding the role and importance of advanced technologies, by the assessment of the process performances and capabilities for manufacturing high quality materials by additive manufacturing and appropriate testing and characterization.

2. OBJECTIVES OF THE ACTIVITY

The activity aimed the development and integration of COMOTI’s capabilities and expertise toward space industry requirements regarding the development of an advanced manufacturing process route and the characterization of the material produced by selective laser melting. The project focused on performing the manufacturing process assessment using the Lasertec 30SLM machine and the material evaluation in order to establish the optimized process parameters for producing high density and appropriate mechanical properties for Inconel 625 Ni-based superalloy, through:

- Assessment of process performances and capabilities for manufacturing high quality materials by SLM metal additive manufacturing and appropriate testing and characterization.
- QA&PA Development and/or gap filling to ensure the process repeatability and reliability.

- Integration of COMOTI's capabilities regarding the development of an advanced manufacturing process route to meet space industry requirements.

3. RESULTS AND DISSCUSION

3.1. PROCESS APPROACH - PROCESS PARAMETERS DEFINITION

SLM capabilities and limitations to produce high density material were evaluated based on state-of-the-art as a solid base of information for the purpose of the project. In particular, the performances and capabilities of Lasertec 30 SLM - ytterbium fiber laser machine were assessed in order to define the adjustable process parameters within the experimental work. –What differentiates the machine from others consists in the replug powder module that includes the sieving unit in a closed-loop with metal powder feeding and recirculation. Unlike many other powder bed fusion machines Lasertec 30 SLM machine exhibits high flexibility of adjusting the process parameters for different parts during the same job.

The influence of process parameters on the densification level of the material was assessed by density measurements on specimens having the dimensions 10 x 10 x 20 mm^3 built in vertical position as shown in Figure 1. The specimens were produced using supporting structures to facilitate the removal from the building plate. All specimens were manufactured with NO CONTOUR using IN 625 metal powder with particle size 15 – 45 µm, D_{50} = 30 +/- 5 µm produced by LPW.

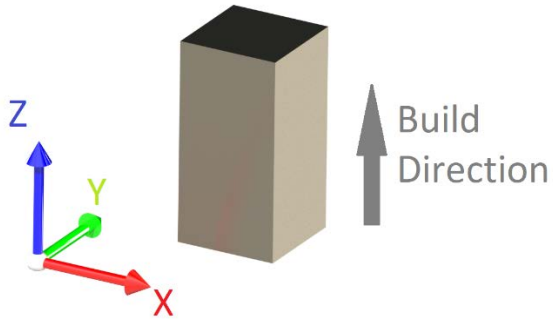

Fig. 1. Specimens used for investigations

Since the density of an alloy is primarily determined by its chemistry, the theoretical density of the investigated IN 625 alloy was calculated using the elemental densities of the alloying elements. Based on the current composition of the alloy a theoretical density of 8.49 g/cm^3 was calculated. This value was used as reference to calculate the relative density as a degree of densification of the manufactured material. The bulk density of the specimens was measured by Archimedes method, according SR EN ISO 3369:2010 standard, using an analytical balance Pioneer PX224 (Ohaus) with a density measurement kit for solids and high purity Ethanol as fluid.

The porosity of the produced material was assessed on specimens using light optical microscopy images made at lower magnification (100x) on 10 micro areas of 3.5 mm^2 each. A binarization technique was achieved by adjusting the brightness and contrast of the image in order to highlight the pores. The technique consisted in converting the

images in 16-bit greyscale format followed by conversion into black and white threshold images. For porosity quantification SCANDIUM software was used.

Adjustable process parameters of Lasertec 30 SLM machine were progressively considered in a first step to define the workspace for material consolidation. The design of experiments focused first on the definition of Laser power – Scanning speed workspace in order to generate high density material, and then to refine it with Layer thickness and Hatch distance as variables.

The experiments were performed within a range of 150 W – 400 W for Laser power and 500 mm/s – 1,000 mm/s Scanning speed, the layer thickness (50 µm) and hatch distance (0.1 mm) being kept constant. Two jobs were performed to produce the same size specimens using scanning patterns of 90° and 67°. For the scanning pattern 67° an additional scan speed was used for all power levels to manufacture specimens at a higher speed (1,000 mm/s), excepting the value of 150 W.

Density measurements of the specimens shown that in both cases (scan pattern 90° and 67°) the density generated at lower Laser powers (150 W and in a good extent 200W) sharply drop as the scanning speed increases.

The porosity measurements on light optical microscopy images taken on samples metallographically prepared and unetched showed that laser power has a strongly influence on reducing the porosity level as the power increase. At low laser powers, the increase of scanning speed leads to the sharp increase of porosity mainly due to the lack of fusion. For the other laser power levels, the increase of scan speeds still generates an increase of measured porosity, but to a lesser extent. This was explained by the mechanism of pores formation. For all low laser powers and scanning speeds, porosity is generally determined by the incorporation of gas bubbles (keyhole porosities), while at high speeds porosities are generated because of lack of fusion. Figure 2 presents by comparison the relative density versus scanning speed for samples manufactured with the lowest laser power (150 W) and of that manufactured with a laser power of 250 W that presents a reasonable level of porosity. In both cases light optical micrographs are presented for low, medium and high scanning speeds.

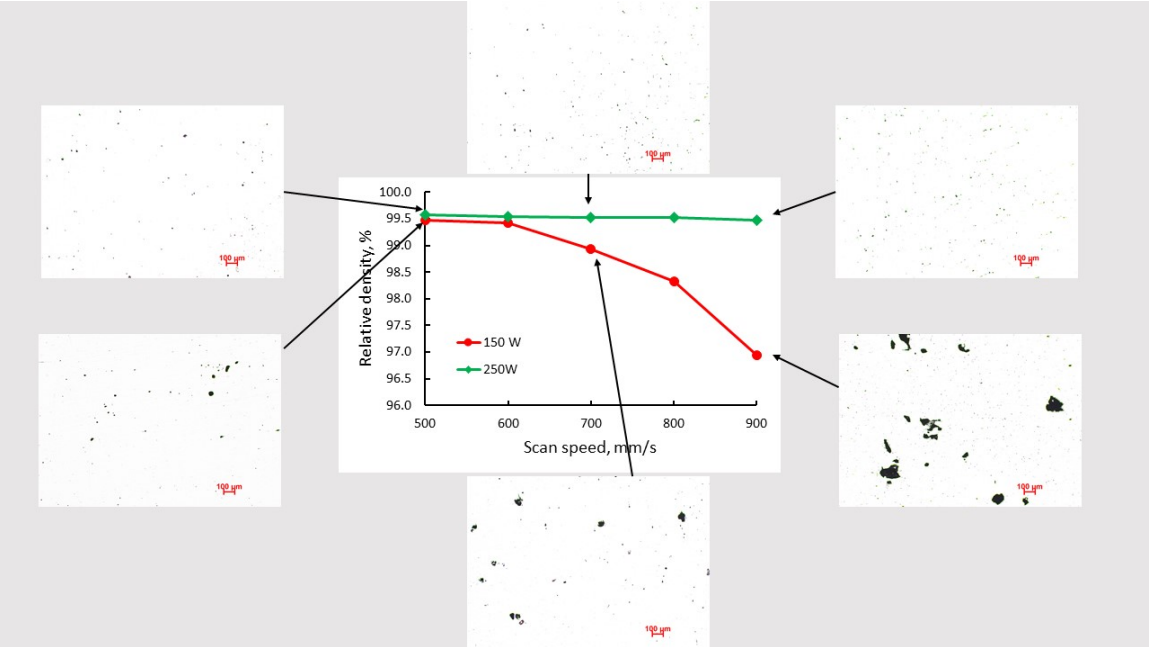

Fig. 2. Micrographs showing the porosity size and distribution measured for two laser powers as a function of scanning speed

A comparison of porosity level of the samples microscopically measured and calculated from density results was done as a function of Volume Energy Density (VED) -Figure 3.

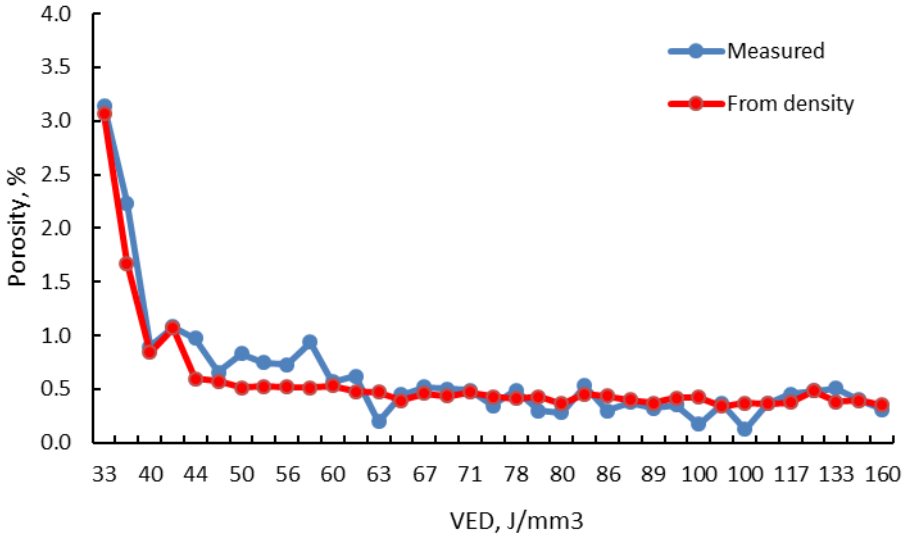

Fig. 3. Measured and calculated porosity vs. VED

Between the metallographically measured porosity and that based on the relative density calculated from densities measured by Archimedes' method there are significant differences. No direct correlation can be done between the porosity levels measured/calculated by the two methods. Metallographic method gives information on the density of samples in the cutting plane and selected micro-areas. Furthermore, small scratches and indentations of the abrasive used for sample preparation could be quantified as porosity.

Porosity calculation based on the density measurement by Archimedes' method take also into account the possible entrapped unmelted metal powder into the pores result of the

lack of fusion. Simply density measurement will not give any information on morphology of porosities mode of formation (keyhole porosities, lack of fusion, etc.). However, Archimedes density provide a rapid assessment of a sample concerning the porosity level.

In order to manufacture as dense as possible high-quality alloy, free of contamination, a Laser power/scanning speed workspace was optimized taking into account the above density measurements results and the need to eliminate or to reduce as much as possible process sources of contamination. As is schematically presented in the Figure 4 this workspace must fulfil simultaneously several conditions:

- avoid or reduce as much as possible the smoke production and spatters;
- avoid or reduce the alloy vaporization;
- avoidance of those sets of parameters that generate sharp decrease of density and lack of fusion.

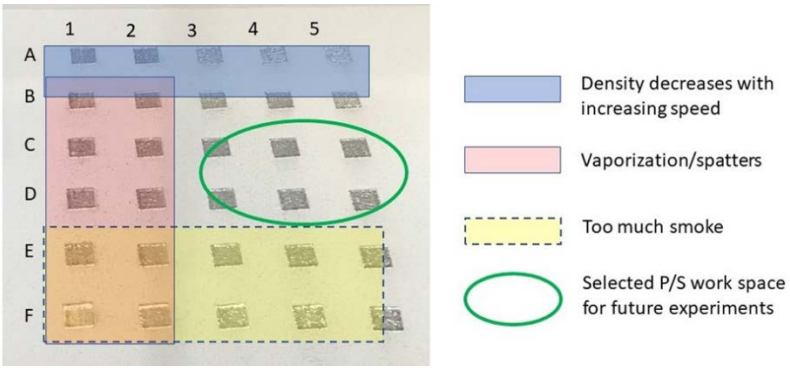

Fig. 4. Laser power/scan speed workspace optimization

Based on the density measurements and process constrains regarding cross contamination of parts and/or of the powder bed the appropriate workspace for the particular alloy investigated was considered for 250 W/300W Laser power and scanning speeds over 700 mm/s.

These process parameters were further used in connection with layer thickness (30 μm, 50 μm and 70 μm) and hatch distance (0.09 mm. 0.1 mm, 0.11 mm and 0.12 mm). Considering the layer thickness, as well as the hatch distance, as variable parameters for two scanning patterns (90° and 67°), it was concluded that 250 W laser power generates more consistent relative density results for both scanning patterns. Layer thickness has a less significant influence on density than laser power/speed. However, the relative density increases as the layer thickness is reduced. For 250 W laser power and 700 – 800 mm/s scanning speed, layer thicknesses in the range of 30 – 50 μm leads to relative densities over 99.5% irrespective of the scan pattern used. By further increase of the layer thickness relative density decreases. An average value of 40 μm was found to be a very reasonable compromise between relative density, surface roughness and the parts building duration.

The general trend of the hatch distance influence is that the relative density increases with the increase of hatch distance from 0.09 mm to 0.11 mm, and then it tends to decrease with the further increase of the hatch distance. This behaviour is mainly due to smaller overlap of the melt tracks at higher hatch distances that can induce lack of fusion porosities and the reduction of relative density.

The hatch distance influence on melt pool shape was investigated on the same type of specimens manufactured using only one direction scanning strategy parallel to Y axis. Each layer was rotated with 180° against the previous one. SEM investigation of the melt pools was performed in order to evaluate the melt pool width and penetration depth as presented in Figure 5, as a function of hatch distance.

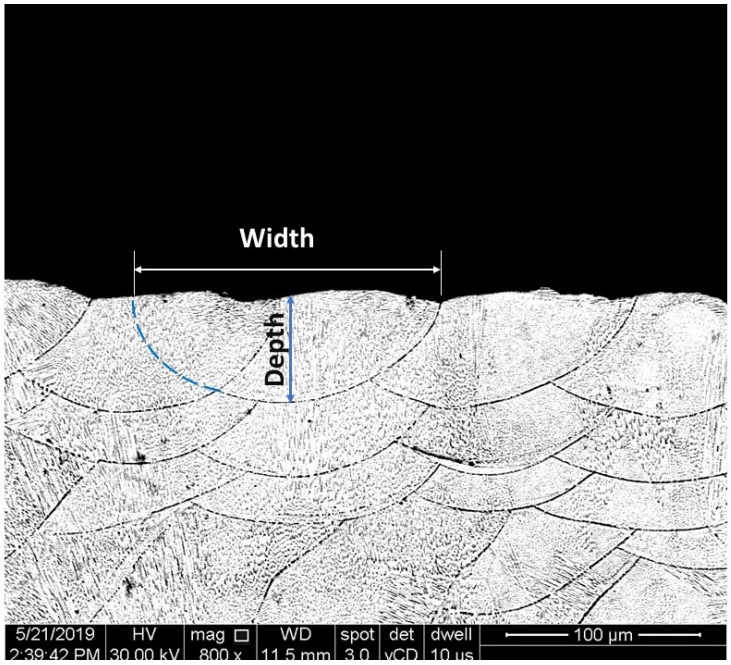

Fig. 5. SEM measurement of melt pool width and depth of penetration

Since the hatch distance influences the volumetric energy density (VED), Figure 6 presents the melt pool characteristic (dept/with ratio) as a function of VED. It can be observed that depth/width ratio decreases with increasing VED.

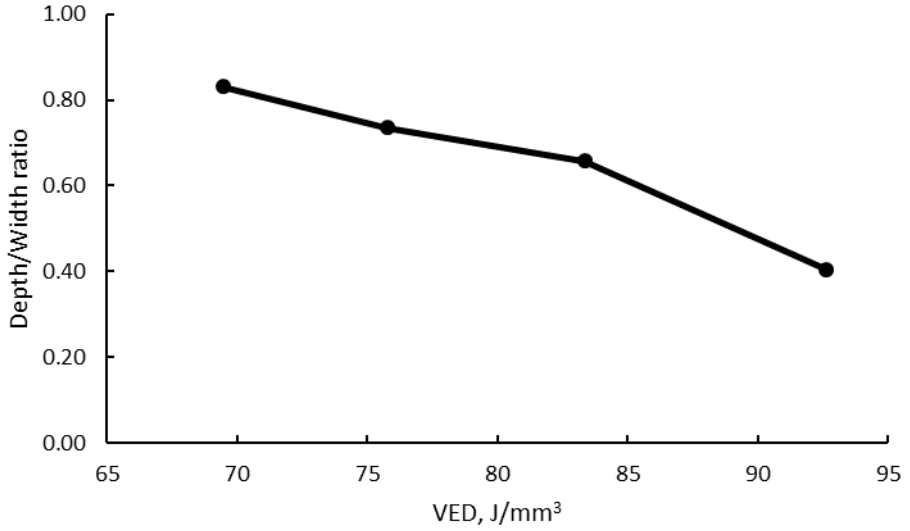

Fig. 6. Depth/width ratio as a function of VED

Other material characteristics such as surface roughness and material density were also evaluated in connection with the process parameters. It was found that the surface roughness decreases as the VED increases (layer thickness decrease). However, no

obvious trend between roughness and scanning speed was noticed. Roughness alone might not be a good indicator such as relative density, as for more complex shapes it largely depends on the positioning of the surface on which roughness is measured. Similarly, hardness measurements of manufactured parts with different layer thicknesses did not shown any marked influence of the scanning speed on hardness.

For the process fine-tuning purpose scanning strategy and Laser focus were used as variables. The scanning strategy was assesses using constant process parameters: Laser power (250 W), Laser speed (750 mm/s), Hatch distance (0.11 mm) and Layer thickness (40 μm). Several scanning strategies were used as presented in Figure 7. By density measurements it was concluded that 90° and strip scanning strategies generate relative densities over 99.5%, while both chessboard strategies generate lower relative densities.

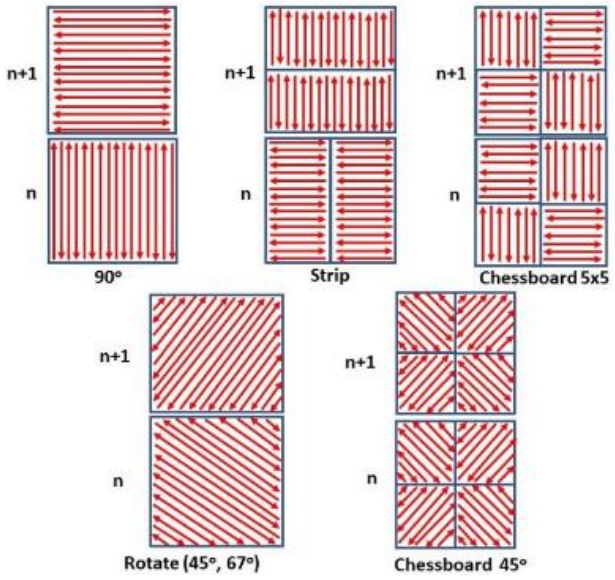

Fig. 7. Scanning strategies

Parts distortion as a function of different scanning strategies were investigated by 3D laser surface scanning to analyze the change of samples surface profile before and after cutting from the building plate. For this purpose, bridge-type test pieces (Figure 8) were manufactured using different scanning strategies: 90°, 67°, strip and 90° chessboard. Pairs of test pieces for each scanning strategy have been built parallel to X and Y axes. All test pieces were first measured on the building plate. One test piece from each pair was cut to be analyzed in the as-built condition and the other was left on the building plate to be subject of stress relieving heat treatment.

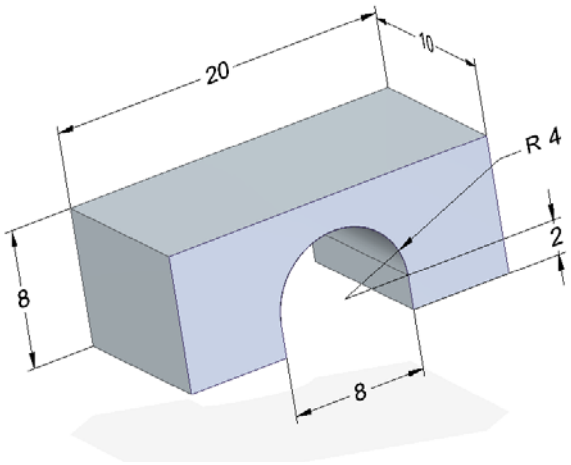

Fig. 8. Bridge-type test piece used for distortion measurements

The 3D laser surface scanning was performed using a “NIKON Altera 10.10.8” coordinate measuring machine with a non-contact NIKON LC15Dx laser scanning probe. Figure 9 presents the surface topography and the height profiles of samples built using a 90° Scanning strategy.

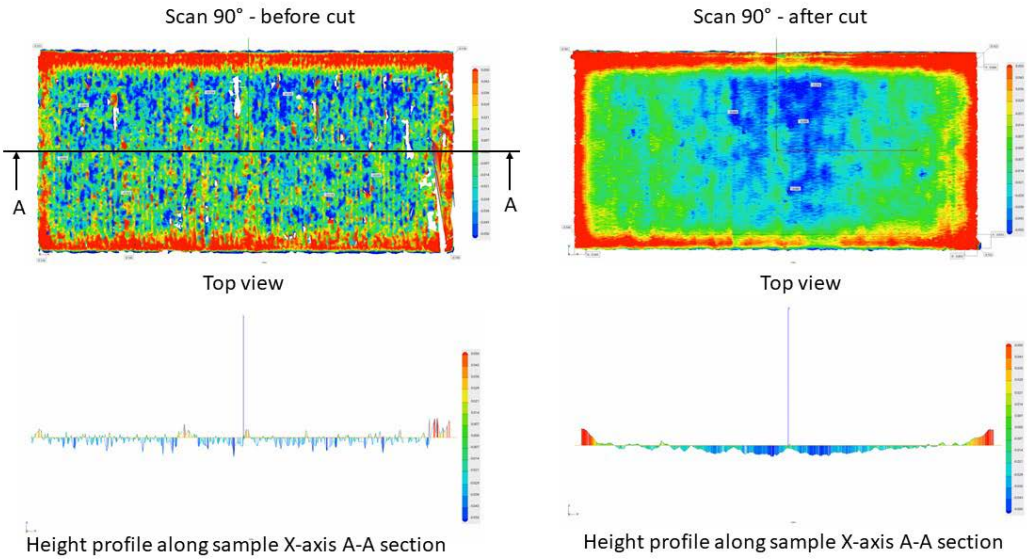

Fig. 9. Height profiles of samples built using a 90° Scanning strategy

Using the FOCUS 2019 machine software, data were post processed and numerically extracted and exported to excel for quantitative analysis of the specimen distortion. The distortion of the as-built test pieces was assessed by calculating the slopes of the curves in the two halves of the sample relative to the symmetry axis and conversion to angles. At least for as-built test specimens manufactured in parallel direction with X-axis of the machine it was found that the smallest distortions are induced by 90° and 90° strip scanning strategies. These are followed in order by 67° and Chessboard 90° scanning strategies.

Laser defocusing was investigated in order to assess the influence on melt pool shape and densification of the produced material. For experimental purposes negative (-0.5 mm, -0.3 mm) and positive (+0.3 mm, +0.5 mm) defocusing distances were used. The

specimens were manufactured using only one direction scanning strategy parallel to Y axis. Each layer was rotated with 180° against the previous one. Macroscopic photographs of the manufactured samples are presented in Figure 10.

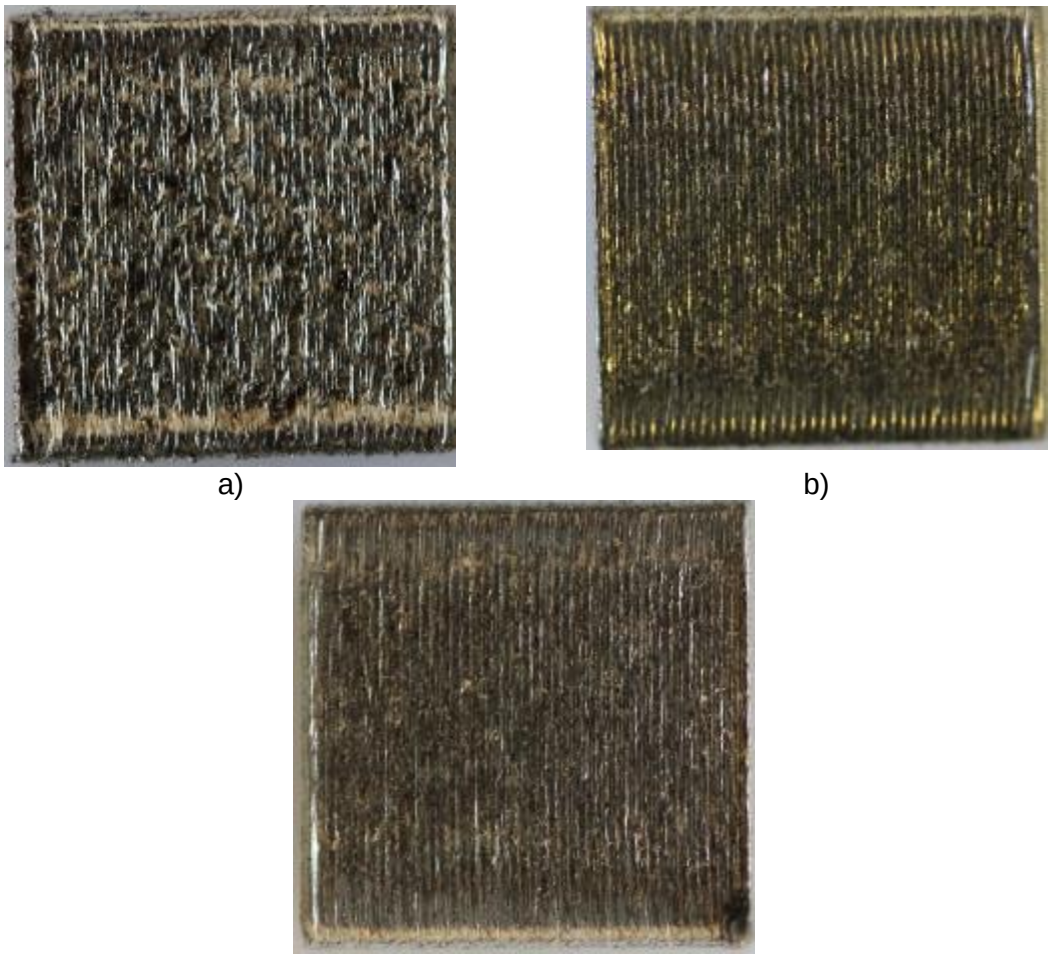

a) b) c)

Fig. 10. Macroscopic view of specimens manufactured with different defocusing distance: -0.5 mm (a), +0.5 mm (b) and 0 mm (c). Actual size 10 x 10 mm^2.

The melt pools investigation shown the tendency of melt pools to become wider and thinner as the negative defocusing amount decrease, while density measurement on samples manufactured with different defocusing amounts has also shown that for the single direction scanning strategy used, higher relative densities are produced with negative defocusing amounts at lower width/depth ratios. However, as the beam defocus acts in only one direction the influence on the parts densification seems to be appropriate only for very simple one direction scanning strategy.

3.2. METAL POWDER CHARACTERIZATION

In order to assess the process repeatability, the goal was to set up a process route to characterize the IN 625 metal powder used for test specimens manufacturing. In this respect it was established a procedure to check the main properties of the commercially available metal powder recommended by the machine vendor on both virgin powder and recirculated powder by the machine.

For this purpose, the following characteristics of the virgin and recycled metal powders were investigated:

- physical properties of the powders:
  - powder morphology and powder particle surface quality;
  - particle size distribution;
  - oxidation state.
- technological properties of the powders:
  - apparent density;
  - tapped density;
  - rheological characteristics - flowability of the powder (flow rate, determination of Hausner ratio - HR and angle of repose - AOR).

3.3. ANCILLARY PROCESS AND VERIFICATION

3.3.1. HEAT TREATMENT

Preliminary heat treatment experiments performed aimed primarily to establish an efficient stress relieve heat treatment and to avoid deleterious phases formation (especially δ-phase). In order to investigate the susceptibility of the alloy to promote deleterious phases formation heat treatment experiments were performed at 700°C, 800°C and 900°C with a longer soaking time of 4 hours, followed by rapid cooling in water.

The influence of the heat treatment temperature on material hardness shows that both materials respond in the same manner to the heat treatment temperature. In both cases at 700°C the hardness increases and then tends to decrease as the temperature increase. Before the heat treatment both materials have closed values of hardness. Despite the increase of the hardness attributed to the beginning of the precipitation of carbides, the microstructure of the sample heat treated at 700°C do not show any obvious difference, the microstructure being very similar with the as-built condition. However, no precipitated carbides were observed on the grain boundaries.

As the temperature is increased at 800°C the morphology of melt pools still shows a fully dendritic structure, but the melt pool boundary becomes blurred compared to the as-built condition. Samples heat treated at 900°C clearly show the advancing of the blurring process of the melt pools grain boundaries as well as the precipitation of carbides along the recrystallized grain boundaries and the increase of δ-phase fraction. At higher magnification the morphologies of precipitated carbides and of δ-phase are clearly revealed (Figure 11).

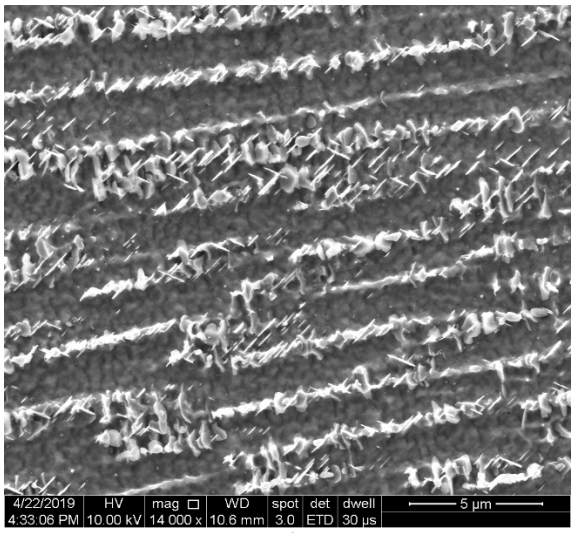

a)

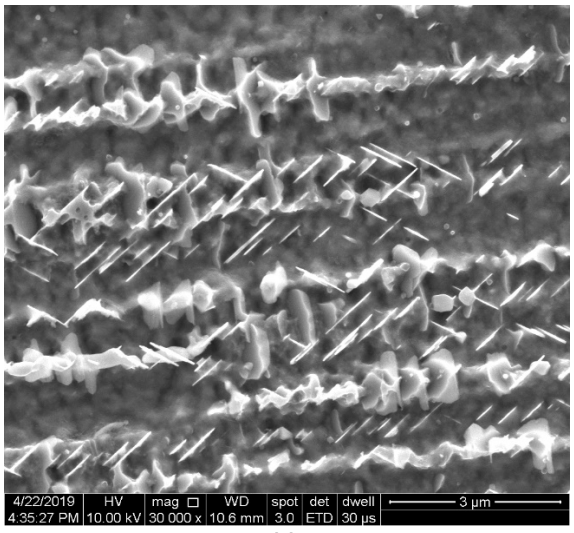

b)

Fig. 11. SEM image of specimen heat treated 4 hours at 900°C: morphology of carbides and δ-phase (a) and needle-like shape of δ-phase (b)

As input for mechanical properties evaluation preliminary heat treatment experiments regarding the material stress relieve have shown that the temperature range between 800°C - 900°C could generates the formation of Nb and Mo rich δ-phase that have to be further removed by a solutioning heat treatment. To avoid this, the heat treatment applied to all tensile test specimens included a stress relieve at 870°C for 1h/air cooling, followed by a solutioning limited at 1000°C not to deteriorate the mechanical strength, with shorter soaking time for 1 hour, followed by rapid cooling (oil quenching) to avoid δ-phase formation. The effectiveness of this heat treatment has been verified by light optical microscopy on samples cut from the ends of tensile test specimens. In all cases the microstructure consists of recrystalized grains (Figure 12).

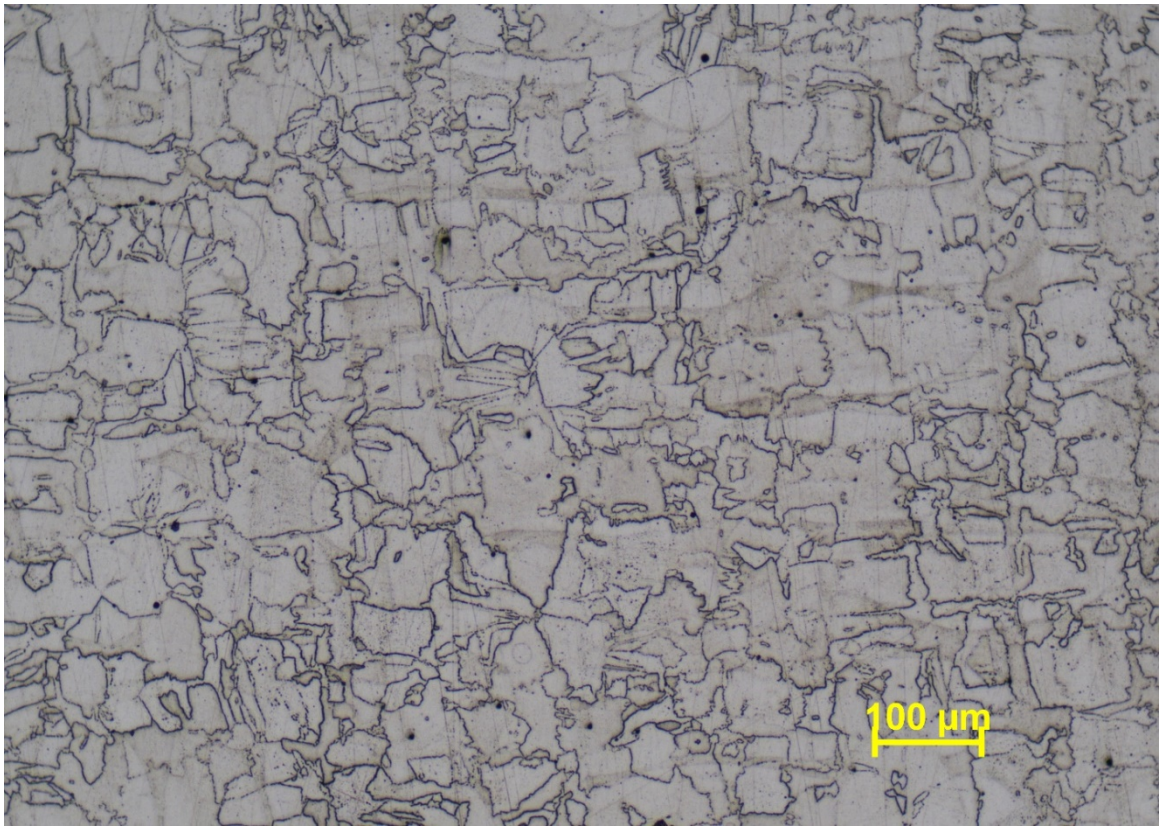

Fig. 12. Optical micrograph of the material in a section parallel with X-Y plane. Etchant: 10 mL HNO3, 10 mL acetic acid, 15 mL HCl and 2–5 drops glycerol

The effectiveness of stress relieve heat treatment was also proved on bridge specimens distortion. The comparative analysis of sample deformations before and after heat treatment showed that a stress relieve treatment conducted at 870°C for 1 h is effective to reduce the residual stresses level. Figure 13 present the profiles of the bridge samples built along Y-axis with a 67° scanning strategy after cutting from the building plate in as-build (AB) and stress relieved (SR) condition.

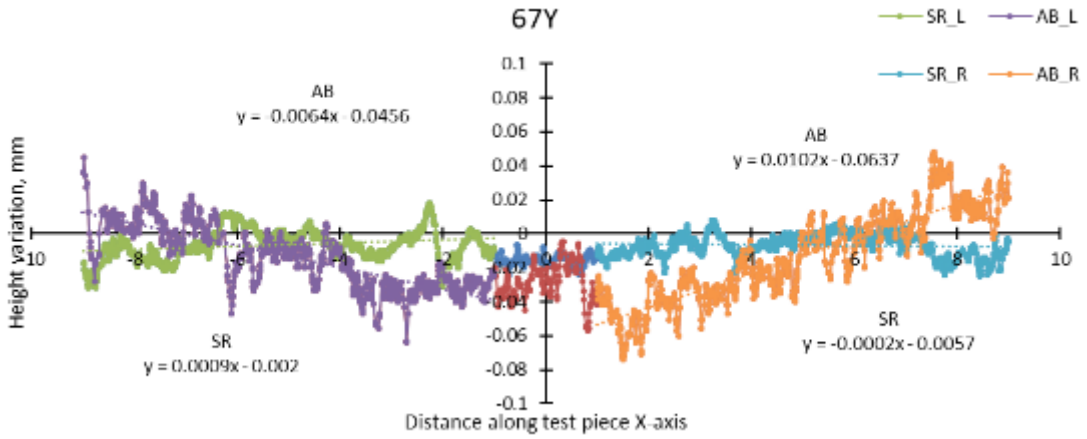

Fig. 13. Comparison of height profiles of test pieces build in Y direction with 67° scanning strategy and associated slopes (half left – L, half right – R)

Because post-processing heat treatment aim to change the material microstructure, the influence on density and porosity were verified. Density measurements were done on specimens in as-built condition and after the heat treatment together with the tensile test coupons. The measurements show that in all cases the relative density depreciates in some respect after the heat treatment from 99.5 – 99.6% in as-built condition to 99.4 – 99.5% after the heat treatment as a result of thermally induced pores formation. Pores formation or growth during heat treatment are generally attributed to the local plastic deformation induced by the entrapped gas expansion during heating. Entrapped gas porosities of 30 – 40 μm in diameter were highlighted.

3.3.2. SUPPORT STRUCTURES

Another way to compensate parts distortion, to increase heat dissipation, to more precise remove the parts or to prevent cracking and delamination of SLM parts due to high residual stress is to proper optimize the support structures. Activities related to support structures were conducted in different directions (support generation in different software or best build orientation) with the main objective to reduce the amount of connections of support structures to the part in order to easier remove it from the building plate and to minimize its impact on the contact surfaces.

For this purpose, five types of support structures were used for simplification and better understanding of their effects on the manufactured parts. The visual inspection revealed that in order to optimize the support structure and to ease removal of the pieces from the building plate, thinner and rarer threads using a lower laser power (130 W) is the best approach. This support type was tested on Bridge-type specimens manufactured parallel to the X and Y-axes and using the scanning strategies 90°, 67° strip and 90° chessboard. For higher laser power the support structure strongly fixed all the parts to the building plate without any detachment too. However, this strong anchoring makes very difficult the mechanical removal of the test pieces from the building plate.

3.4. MECHANICAL TESTING

During Process adjustment and fine-tuning activities several process parameters were assessed in order to produce high density material. Based on the experimental results, the

optimized process parameters to be used for tensile test Specimen Manufacturing and Material Evaluation were defined as follows:

- Laser Power: 250 W
- Scanning speed: 750 mm/s
- Layer thickness: 40 µm
- Hatch distance: 0.11 mm
- Focus: 0
- Scanning strategy: 90° rotate

The material mechanical properties assessment against specimen orientation in the building volume considered the room temperature tensile testing of fully heat-treated specimens. For manufacturing the tensile test specimens, cylindrical bars of 10 mm in diameter and 80 mm long were designed to be manufactured in 3 different orientations: along X-axis, Y-axis, Z-axis, and tilt with 45° in the Z-X plane as shown in Figure 14. For each orientation 9 specimens/job were manufactured in 3 different jobs/orientation. The specimens oriented parallel to X and Y-axis were built together on the same platform to assess the results in X-Y plane.

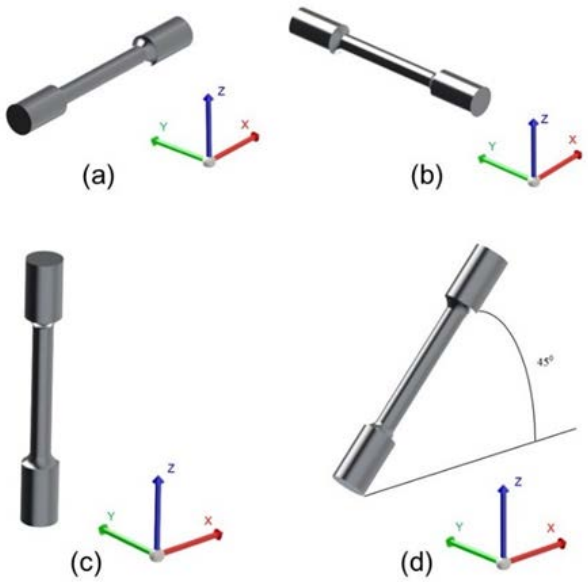

Fig. 14. Tensile test specimens orientation in the building volume: along X-axis (a), along Y-axis (b), along Z-axis (c) and tilt with 45° in Z-X plane

Tensile testing at room temperature was performed according ISO 68921-1:2009 using an electromechanical universal testing machine, Intron 3369 Dual Column Testing System, with a maximum 50 kN load capacity. During the tensile testing the strain rate over the parallel length was set to $\dot{e}_{Lc}$= 0,00025 s^{-1} until the detection of the yield strength. After determination of the yield strength the extensometer was removed and the strain rate over the parallel length was changed to $\dot{e}_{Lc}$= 0,0067 s^{-1}.

The analysis of all tensile tests data shows no significant differences between the average of all results obtained on specimens built along X and Y - axis for tensile strength, yield strength and Young modulus. The elongation and reduction of area of specimens built along Y – axis is to a lesser extent smaller than the results obtained for specimens along

X-axis. Although the average values of elongation and reduction of area for both X and Y orientation are over the minimum specification of ASTM F3056-14, a limited number of results for reduction of area for both orientations (X and Y) fall below 30%, respectively 3 out of 35 results for the X-axis and 4 out of 36 results for the Y-axis. Excepting only one out of 36 results on Y-axis, the elongation of all specimens built along X-axis and Y-axis are over the specification limit (30%).

The comparative analysis of all tensile test results on specimens built in vertical position (along Z axis), tilt at 45° in X-Z plane and in horizontal position along X and Y - axis shows that test pieces built in vertical position have lower tensile strength and yield strength, but higher reduction of area than all the other orientations. The elongation at rupture for the specimens built in Z direction is in some extent higher than the elongation of the specimens built tilt at 45° in X-Z plane. The specimens built in horizontal position exhibit for both X and Y orientations the highest tensile strength and yield strength, but the lower elongation and reduction of area.

Normal to the building direction (X – Y plane) higher yield strength, ultimate tensile strength and Young's modulus, but lower elongation and reduction of area are observed than in parallel direction to the building direction (Z – axis). Generally, the texture resulted from manufacturing process is the major cause of these anisotropic mechanical properties of AM metallic parts.

3.5. PROCESS TRACEABILITY

The traceability system is a risk management tool used to monitor/control the quality of the AM parts realized in COMOTI using LASERTEC 30SLM machine. The additive manufacturing process has different challenges related to the accuracy, reproducibility and reliability of the entire technological flow.

A traceability system was established according to quality assurance methodologies that are used in standard space practice. The traceability system aims to provide the necessary information starting from the procurement and conformity check of the metal powder until the final stage of specimens/parts manufacturing process validation. In this respect COMOTI has developed a traceability system and a series of work instructions, guidelines, registration sheets, check lists and procedures were elaborated and implemented.

4. FOLLOW-ON ACTIVITIES

During the activity COMOTI gained the knowledge and the skills necessary to manufacture high density material by additive manufacturing and to properly address the material testing and characterization. By the fulfilment of this De-Risk activity a TRL 3 was achieved.

The experimental results obtained in the frame of this De-Risk activity are accelerating the development activities in the field of additive manufacturing of fully dense materials and COMOTI's capabilities and expertise toward space industry requirements in the field of metal additive manufacturing. For the post-processing purposes of more complex components, a series of ancillary process were evaluated for removal of support structures, heat treatment, machining, NDI, surface treatment. A local network of service

providers was assessed based on their expertise and capabilities in order to future perform the activities requiring specific expertise not available within COMOTI.

Once the optimum process parameters were established and validated on samples and specimens covering the end-to end process, the future developments and follow-on activities aim to manufacture more complex shape components made by SLM for space applications. As a result of jointly work with ESA-ESTEC follow-on activities were defined within the GSTP activity “Assessing the use of Advanced Manufacturing to improve and expand space hardware capabilities – EXPRO+”